Evaluation of the Solid State Dipole Moment and Pyroelectric Coefficient of Phosphangulene by Multipolar Modeling of X-ray Structure Factors

Georg K. H. Madsen,*[a] Frederik C. Krebs,[b] Bente Lebech,[b] and Finn K. Larsen[a]

Abstract: The electron density distribution of the molecular pyroelectric material phosphangulene has been studied by multipolar modeling of X-ray diffraction data. The "in-crystal" molecular dipole moment has been evaluated to 4.7 D corresponding to a 42% dipole moment enhancement compared with the dipole moment measured in a chloroform solution. It is substantiated that the estimated standard deviation of the dipole moment is about 0.8 D. The standard uncertainty (s.u.) of the derived dipole moment has been derived by splitting the dataset into three independent datasets. A novel method for obtaining pyroelectric coefficients has been introduced by combining the derived dipole moment with temperature-dependent measurements of the unit cell volume. The derived pyroelectric coefficient of $3.8(7) \times 10^{-6}\,\mathrm{C\,m^{-2}\,K^{-1}}$ is in very good agreement with the measured pyroelectric coefficient of $p = 3 \pm 1 \times 10^{-6}\,\mathrm{C\,m^{-2}\,K^{-1}}$. This method for obtaining the pyroelectric coefficient uses information from the X-ray diffraction experiment alone and can be applied to much smaller crystals than traditional methods.

Keywords: dipole moment · electron density distribution · materials science · pyroelectricity · X-ray scattering

Introduction

The control offered by synthetic organic chemistry makes the field of molecular materials an interesting and rapidly expanding area of research. Molecular materials with specific properties may be synthesized for use in electronic and optoelectronic devices.[1] Pyroelectricity is such a solid state electronic property.[2, 3] It depends on the presence of a polar axis in the unit cell, which may set up a permanent electric polarization, even in the absence of an external field. The material shows a pyroelectric effect if a change in temperature creates a change in the spontaneous polarization.

$$\Delta P = p\,\Delta T \qquad (1)$$

where p is the pyroelectric coefficient. In molecular pyroelectric materials the molecular structure most often does not change significantly with temperature. This means that a temperature dependent pyroelectric coefficient can be calculated from the unit cell dipole moment and the change in unit cell dimensions.

In the present work we will use experimental X-ray structure factors to evaluate the solid state dipole moment of a molecular pyroelectric material, phosphangulene, which recently was synthesized and considered for use in infrared detection.[4] Phosphangulene, Figure 1, crystallizes in the polar space group $R3m$ and the individual molecules have the same symmetry as the point group of the unit cell with the central phosphorous atom lying on the threefold axis. This symmetry means that the molecular dipole moment, μ, is colinear with the polar axis, Figure 2. If the unit cell volume

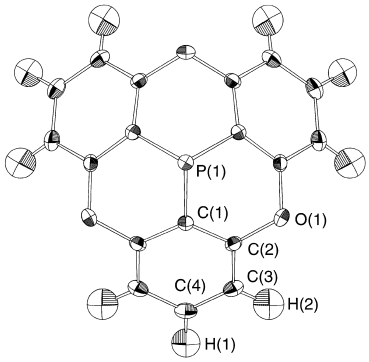

Figure 1. ORTEP drawing of phosphangulene showing the atom numbering scheme and 90% ellipsoids.

[a] Dr. G. K. H. Madsen, Prof. F. K. Larsen
Department of Chemistry, University of Aarhus
8000 Århus C (Denmark)
Fax: (+45) 86196199
E-mail: georgm@kemi.aau.dk

[b] Dr. F. C. Krebs, Prof. B. Lebech
Condensed Matter Physics and Chemistry Department
Risø National Laboratory, 4000 Roskilde (Denmark)

Supporting information for this article is available on the WWW under http://www.wiley-vch.de/home/chemistry or from the authors.

  0947-6539/00/0610-1797 $ 17.50+.50/0

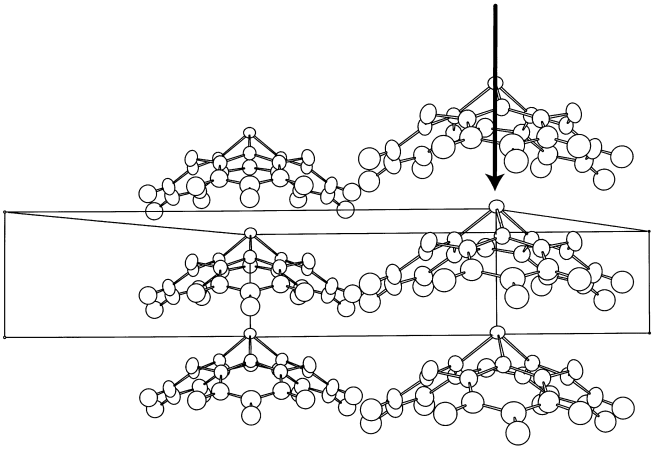

Figure 2. ORTEP drawing of two molecular stacks and the unit cell. The direction of the molecular dipole moment (following the convention that the arrow goes from negative to positive) is shown with an arrow on a molecule.

changes linearly with temperature ($V(T)=aT+b$) and the molecular dipole moment is considered independent of temperature, the pyroelectric coefficient is given as[4] where Z is the number of molecules in the unit cell.

$$p=\frac{dP}{dT}=-\frac{Za}{(aT+b)^2}\begin{pmatrix}0\\0\\\mu\end{pmatrix} \tag{2}$$

Spackman has reviewed the derivation of molecular dipole moments from both experimental diffraction data,[5] and theoretically calculated structure factors.[6] It was concluded that, in general, quite reliable molecular dipole moments can be derived from multipolar modeling of diffraction data. A big advantage of estimating electrostatic moments from X-ray diffraction data is that both the size and the direction of the solid state molecular dipole moment is obtained. In pyroelectric materials the permanent electric field over the crystal is expected to induce an enhancement of the molecular dipole moment compared with the gas-phase value. Therefore the dipole moments from gas-phase ab initio calculations are not necessarily a good approximation of the "in-crystal" molecular dipole moment.

A prerequisite for a material to exhibit pyroelectric properties is that it belongs to a polar space group. This unfortunately complicates the modeling of the measured structure factors because of more ambiguity in-phase assignments of the reflections for the non-centrosymmetric space group than in the centrosymmentric case. Phosphangulene represents a challenge because it crystallizes in the non-centrosymmetric high symmetry space group $R3m$, with five of the eight atoms on special positions in the asymmetric unit.[7, 8] However, obtaining pyroelectric coefficients from diffraction data has advantages. First of all, the testing of a newly synthesized material requires solving the crystal structure anyway. With the advent of area detector diffractometers for rapid data collection, a multipolar derived pyroelectric coefficient can therefore be obtained with a modest amount of extra experimental effort. Furthermore, it is noteworthy that the method, contrary to traditional methods,[4] can be applied to small crystals with volumes of a few thousandths of a mm^3, the size of the single crystal normally used in an X-ray study of the crystal structure.

Abstract in Danish: *Elektrontæthedsfordelingen i det molekylære pyroelektriske materiale phosphangulen er blevet undersøgt ved multipolmodelering af røntgendiffraktionsdata. Det molekylære dipolmoment i fastfase er blevet evalueret til 4.7 D, hvilket svarer til en 42 % forøgelse af dipolmomentet sammenlignet med dipolmomentet målt i en kloroformopløsning. Det er godtgjort, at den estimerede standardafvigelse på dipolmomentet er omkring 0.8 D. Det udledte dipolmoment er blevet kombineret med temperaturafhængige målinger af enhedscellevolumet til beregning af den pyroelektriske koefficient. Den herved beregnede værdi på $3.8(7)\times10^{-6}\,C\,m^{-2}\,K^{-1}$ viser en meget god overensstemmelse med den målte pyroelektriske koefficient på $p=3\pm1\times10^{-6}\,C\,m^{-2}\,K^{-1}$. Denne metode til udledelse af den pyroelektriske koefficient bygger alene på information opnået fra røntgendiffraktionseksperimentet og kan anvendes på meget mindre krystaller end traditionelle metoder behøver.*

Multipolar modeling of X-ray data

The program XD[9] was used for the multipolar modeling of the X-ray diffraction data. In the multipolar model the atomic density contributions are parametrized into a core term, ρ_{core}, a spherical valence term, $\rho_{valence}$, and a set of multipolar functions.[10]

$$\rho_{atom}(r)=P_{core}\rho_{core}(r)+P_{valence}\kappa^3\rho_{valence}+\sum_{l=0}^{l_{max}}\kappa_l'^3R_l(\kappa_l')\sum_{m=0}^{l}P_{lm\pm}d_{lm\pm}(\theta,\phi) \tag{3}$$

In this equation $d_{lm\pm}$ values are angular functions and R_l are the Slater type radial functions, where n_l and ζ_l can be chosen

$$R_l(r)=\frac{\zeta_l^{n_l+3}r^{n_l}}{(n_l+2)!}\exp(-\zeta_l r) \tag{4}$$

for each value of l. The scattering factors of each atom are modified by refining the κ expansion/contraction coefficients and populations, P, of the individual functions.

The multipole model partitions the electron density into pseudo-atomic fragments that each contribute to the total molecular dipole moment. The total molecular dipole moment can be calculated as a sum over the pseudo-atomic charges and dipole moments where the pseudo atomic charges

$$\mu=\sum_i\mu_i+\sum_i r_i q_i \tag{5}$$

are defined as $q_i=Z_i-P_{core}-P_{valence}$. The atomic dipole moments can be calculated from the atomic dipole populations.[10]

$$\mu_x=\int P_x d_{11+}R_1 x\,dr=-\frac{20}{3\kappa_1'\zeta_1}P_x \tag{6}$$

where P_x is a linear combination of P_{10}, P_{11+}, and P_{11-}, that depends on how the local atomic coordinate system

0947-6539/00/0610-1798 $ 17.50+.50/0 *Chem. Eur. J.* **2000**, *6*, No. 10

is oriented with respect to the molecular coordinate system.

With nine hydrogen atoms bonded to electron attracting phenyl rings, the C–H bond dipoles will be decisive for the molecular dipole moment. As the hydrogen atoms have no core electrons, their κ expansion/contraction coefficients will be correlated with their atomic displacement parameters. Furthermore, the bond directed dipoles of the multipole model will be correlated with the C–H bond distances. To obtain unbiased positional and vibrational parameters for the hydrogen atoms, it was decided to determine these through a neutron diffraction study. Because of the high molecular and crystal symmetry we attempted to use neutron powder diffraction. The actual influence on the derived dipole moment of introducing the hydrogen parameters obtained by neutron diffraction was only small. This is discussed in more detail under the Experimental Section.

Further discussion of the modeling procedure can also be found in the Experimental Section. Here we only report the results of what we consider to be the best model. The molecular dimensions are reported in Table 1 and Table 2,

Table 1. Bond distances found in the X-ray study with the hydrogens placed at the positions determined in the neutron study.

Bond	Å
P(1)–C(1)	1.8027(6)
O(1)–C(2)	1.3951(6)
C(1)–C(2)	1.3902(5)
C(2)–C(3)	1.3913(6)
C(3)–C(4)	1.3996(6)
C(3)–H(2)	1.08(1)
C(4)–H(1)	1.06(1)

Table 2. Bond angles found in the X-ray study with the hydrogens placed at the positions determined in the neutron study.

Bond	°
P(1)-C(1)-C(2)	119.9(1)
C(2)-O(1)-C(2)	115.1(1)
O(1)-C(2)-C(1)	120.0(1)
O(1)-C(2)-C(3)	119.5(1)
O(1)-C(2)-C(1)	120.0(1)
O(1)-C(2)-C(3)	119.5(1)
C(2)-C(3)-C(4)	118.5(1)
C(2)-C(3)-H(2)	120.4(4)
C(3)-C(4)-H(1)	119.3(4)

and the static deformation density in the plane of the phenyl ring is shown in Figure 3. An isosurface plot of the static deformation density is shown in Figure 4, depicting the lonepair on the phosphorous atom and the bonding densities. The pseudo atomic charges and contributions to the molecular dipole moment are given in Table 3, but the values should be interpreted with some caution. The division of a molecule into atomic fragments based on a multipole model is notoriously flawed, especially when employing flexible radial functions. However, to properly model the *total* density the model needs to have sufficient radial freedom.

Table 3. Pseudo-atomic charges and contributions to molecular dipole. q_i is the pseudo-atomic charge. $r_{iz}q_i$ is the contribution of the atomic charge to the z component of the dipole moment and μ_{iz} is the contribution of the atomic dipoles to the z component of the dipole moment.

Atom	q_i (D)	$r_{iz}q_i$ (D)	μ_{iz} (D)	Multiplicity
P(1)	1.88	13.67	– 2.48	1
O(1)	– 0.96	– 1.60	0.09	3
C(1)	– 0.46	– 1.17	– 0.75	3
C(2)	0.36	0.16	– 0.39	6
C(3)	0.08	– 0.24	0.00	6
C(4)	– 0.38	1.72	– 0.17	3
H(1)	0.13	– 0.93	– 0.36	3
H(2)	0.08	– 0.37	– 0.22	6

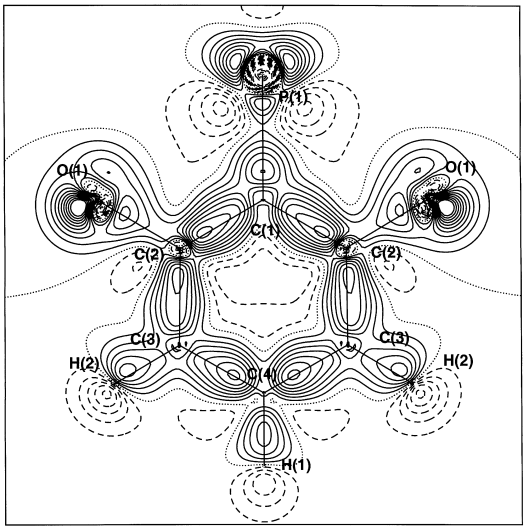

Figure 3. Static deformation map. The contour interval is 0.1 e Å^{-3}. The dotted line is the zero contour. Solid lines are positive contours, broken lines negative contours.

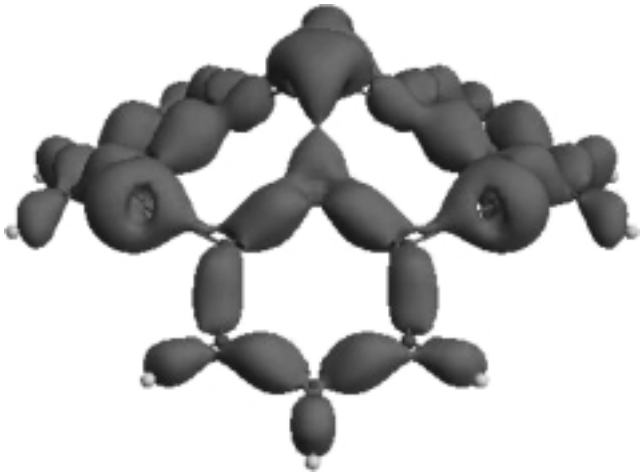

Figure 4. Isosurface plot of the static deformation density. The surface covers the volume with density larger than 0.25 e Å^{-3}.

The important thing is the total density, not the individual atomic fragments that have questionable physical justification.

Results and Discussion

Accuracy of the derived dipole moment: The evaluation of the dipole moment of a molecule in a crystal relies on the partitioning of the crystal into molecular fragments. In the present study the intrinsic division of direct space by the multipole model has been utilized. Many different space partitioning schemes have been proposed[10] and the derived molecular dipole moment can be dependent on the chosen partitioning scheme. This, however, is not the case for phosphangulene because all the dipole moments point in the same direction and the property of interest is the unit cell dipole moment which is independent of the chosen partitioning scheme, as described in Table 7. As mentioned above the molecular dipole moment converges to a value of 4.7(25) D. This corresponds to a dipole moment enhancement of 95% compared with the theoretical ab initio gas phase value of 2.41 D and 42% compared with the value of 3.3 ± 0.1 D measured in a chloroform solution.[12] An induced dipole moment of this magnitude compares well with what has previously been found in polar crystals by other authors.[5, 11] At the experimental geometry a dipole moment of 2.48 D was calculated. The small difference between the gas phase dipole moment at the crystal geometry and the optimized geometry means the dipole moment enhancement arises from a polarization of the electron density in the solid state.

Precision of the derived dipole moment: The very large s.u. on the derived dipole moment is troublesome. If it is to be trusted, the observed dipole moment enhancement is not significant at all. When evaluating the enhancement of the dipole moment when going from gas phase to solid state, we are attempting to gain information on how the electron density distribution of one molecular entity polarizes as a response to the permanent electric field over the crystal. The problem with evaluating such interaction densities is that the s.u. of the experimental electron densities are of similar magnitude. The s.u. reported has been calculated by propagation of the least squares errors on the monopole and dipole populations.[5] This procedure will inevitably lead to very large s.u.'s because of the correlations between the multipole populations. However, the fact that the individual multipole populations have large s.u.'s does not necessarily mean that the total electron density is poorly determined. This is especially true for the more flexible models. Therefore we do not feel that the s.u. value is a realistic estimate of the standard uncertainties. A very recent study by Spackman et al. investigated whether it is possible to obtain reliable interaction densities from multipolar refined diffraction data.[13] The study was based on theoretically calculated structure factors and the underlying electron distribution was therefore known. This study found that multipolar models are very successful in retrieving the interaction density and it was pointed out that interaction densities are not a random but a systematic effect which the multipolar models were capable of retrieving despite the sometimes large s.u.

If the interaction density (and thereby the dipole moment enhancement) is observable, we should be able to conduct a whole series of independent data collections on different phosphangulene crystals and obtain a series of molecular dipole moments statistically distributed around a mean value that is significantly larger than the gas phase value. Doing this in practice would off course be far too time consuming. We do, however, have a crude alternative. Such is the quality of the present data set that we can utilize the high symmetry to split the half sphere of data into three almost complete datasets. Each data set contains one sixth of reciprocal space and the corresponding Friedel pairs. Because of anomalous scattering Friedel pairs may not be averaged. Thus the only averaging is between re-measurements of the same reflections. The three sets of data were refined individually. A short summary of these results are given in Table 4.

Table 4. The results of fitting model (H) to the complete and the three partial data sets.

Dataset	Number of unique reflections	$Rw(F^2)$ (%)	μ (D)
full	1486	3.71	−4.7(25)
1	1478	4.01	−4.0(28)
2	1443	4.18	−5.0(28)
3	1274	4.24	−3.4(28)

The average dipole moment of the four data sets is 4.3 D. Data set No. 3 is less complete than the two other constructed data sets, because the way the DISPLEX is mounted means that certain reflections cannot be reached. But even including this data set the estimated standard deviation of the distribution of derived dipole moments is only 0.8 D. We realize that these four "measurements" are not independent, but we still think that this procedure indicates a more realistic estimate of the s.u. on the multipolar derived dipole moment than propagation of least-squares errors.

The pyroelectric coefficient: The temperature dependence of the unit cell is shown in Figure 5. Inserting the values $\mu =$ 4.7 D, $a = 0.0850$ Å^{3}K^{-1}, $b = 998.8$ Å^3, derived from Figure 5,

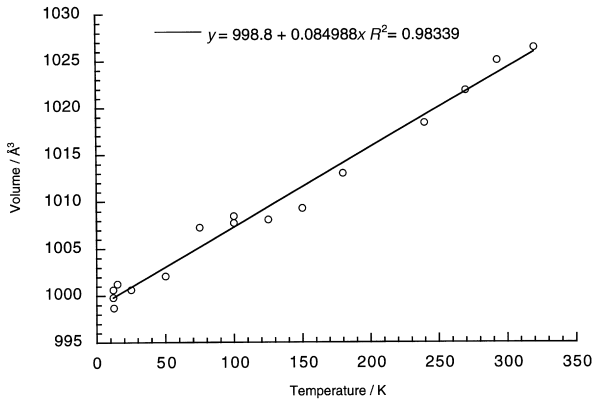

Figure 5. Unit cell volume as a function of temperature. The data in the temperature interval from 180 K to 320 K are from ref. [4].

into Equation (2) we obtain a pyroelectric coefficient at 298 K of $p = 3.8 \times 10^{-6}$ Cm^{-2}K^{-1} in very good agreement with the measured pyroelectric coefficient of $p = 3 \pm 1 \times 10^{-6}$ Cm^{-2} K^{-1}.[12] Propagating an s.u. of 0.8 D on the molecular dipole moment gives an uncertainty of 0.7×10^{-6} Cm^{-2}K^{-1}.

0947-6539/00/0610-1800 $ 17.50+.50/0 *Chem. Eur. J.* **2000**, *6*, No. 10

The direction of the dipole moment: The direction of the dipole moment relative to the molecular framework is shown in Figure 2, and indicates that the phosphorous atom is at the negative end and the hydrogen atoms at the positive end of the molecule. In the present study there is consensus on the direction of the molecular dipole moment as obtained from the ab initio calculations and from the multipolar model. It has to be commented that this direction is opposite to that of the dipole moment published earlier.[4] The previous determination of the molecular dipole moment direction was based on relating the measured macroscopic polarization of phosphangulene crystals of known morphology to that of the absolute molecular configuration, which was found by analysis of Friedel-related reflections.

If the direction of the dipole moment is correctly determined in the present study there must be an error either in the previous measurement of the macroscopic polarization, in the previous determination of the absolute configuration or in the previous assignment of crystal morphology. The measurement of the macroscopic polarization utilized the fact that pyroelectric materials concentrate charges at the surface which oppose the polarization arising from the permanent dipole moment of the unit cell. The method was carefully calibrated on $LiNbO_3$ crystals with known polarization and on every phosphangulene crystal tested, positive surface charges where found at the pointed end of the bullet-shaped crystal, ref.[4] and Figure 6. The determination of the absolute morphology

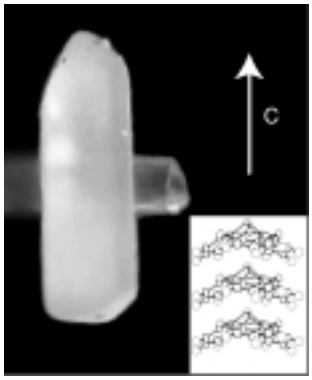

Figure 6. Photograph of a typical phosphangulene crystal put in relation to the absolute morphology.

of the crystal is dependent on the right interpretation of the diffractometer geometry in relation to the crystal geometry. In order to resolve the discrepancy we have re-determined the absolute morphology of three phosphangulene crystals: the original crystal and two new crystals of similar morphology. This was done using data collected on a Siemens SMART area detector diffractometer with $Mo_{K\alpha}$ radiation at 120 K. All three crystals were found to have the same absolute configuration as originally determined, but it was found that the morphology presented previously[4] was in fact in error. The morphology determined for the three instances was the same, namely with the polar *c* axis pointing towards the pointed end of the crystals, which is opposite to the direction previously reported. It is thus concluded that the direction of the dipole moment reported here in Figure 2, is correct and the absolute morphology of the crystal is as shown in Figure 6.

The electrostatic potential: The present study has focused on the size and direction of the phosphangulene dipole moment, because these are the properties that are directly related to the macroscopic properties of phosphangulene. A large number of quantities can be computed from an experimental charge density.[10] One such quantity is the deformation density, Figure 3 and Figure 4. Another is the electrostatic potential given in Figure 7. Figure 7 shows how the electrostatic potential is positive both at the phosphorous atom and at the hydrogen atoms. The molecule therefore also has a significant quadrupole moment and it is not easy to predict the direction of the dipole moment of phosphangulene purely following chemical intuition. To modify a molecular pyroelectric material chemically in a rational way it is important to know the microscopic direction of the molecular dipole moment, not just the macroscopic polarization in the crystal. It is therefore a big advantage of obtaining dipole moments from diffraction data, that the direction of the dipole moment is obtained.

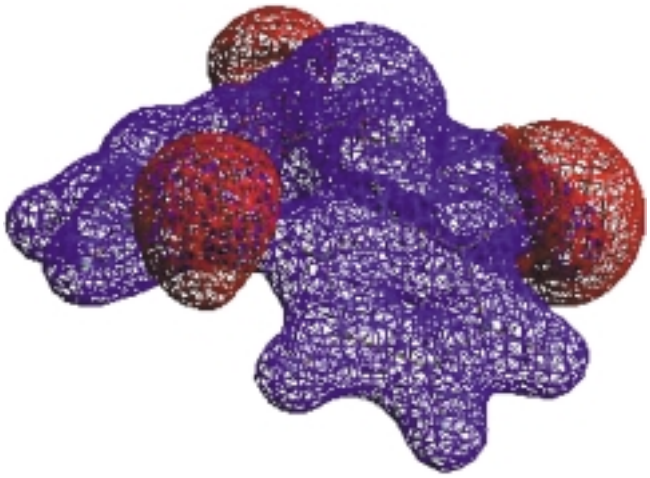

Figure 7. Isosurface plot of the electrostatic potential. The red surface covers a volume with an electrostatic potential smaller than $-0.2\ e\ Å^{-1}$. The blue surface covers a volume with an electrostatic potential larger than $0.4\ e\ Å^{-1}$.

Conclusion

In the present work we have considered the use of multipolar modeling for the evaluation of the solid state dipolar moment of a pyroelectric material, phosphangulene. The solid state dipole moment has been evaluated to a value of 4.7 D with a s.u. of about 0.8 D. The direction of the molecular dipole moment has been determined unequivocally. When the hydrogen atoms sit near the edge of the molecule, and therefore contribute a large amount to the molecular dipole moment, it is important either to obtain supplementary information on the hydrogen positions or to systematically vary the hydrogen positional and displacement parameters within some reasonable limits, in order to estimate the influence on the derived

dipole moment. In the present case we have measured neutron powder diffraction data and found that the use of literature values for average distances in the calculation of the hydrogen positions does not introduce a significant error in the derived molecular dipole moment. However the s.u.'s on the bondlengths obtained from the neutron powder diffraction study are large. If the hydrogen atoms are involved in strong hydrogen bonding neutron diffraction can be necessary to obtain the required accuracy.[14, 15]

Combining the multipolar derived dipole moment with the temperature-dependent measurements of the unit cell volume has allowed us to evaluate the pyroelectric coefficient of solid phosphangulene to $3.8(7) \times 10^{-6}\,\mathrm{C\,m^{-2}K^{-1}}$. The ab initio prediction of crystal structures is still largely an unfulfilled challenge.[16] Therefore the design of new molecular pyroelectric materials continues to involve synthesizing a series of candidates, solving their crystal structures and, if potentially promising, measuring the pyroelectric coefficient of sometimes minute single crystals.[17] The main advantage of extracting pyroelectric coefficients with the method described here is that it can be applied to any crystal suitable for X-ray diffraction. This means that smaller crystals than usual can be screened, thereby facilitating the synthetic procedure.

With the appearance of area detectors and modern integrated program packages such as XD[9] a reasonable quality data set can be obtained and treated in a few days.[18] Multipolar modeling of diffraction data can therefore become a valuable tool with many applications in chemical crystallography. In the present study we have directly related the multipolar derived charge density to a macroscopic observable, namely the pyroelectric coefficient.

Experimental and Computational Methods

X-ray study: Phosphangulene was synthesized and single crystals were grown as described previously.[4] The crystal used for data collection was mounted in a glass capillary which was glued to an aluminium pedestal. A few carbon fibers in the capillary secured good thermal contact between the crystal and the pedestal which was fitted on the cold station of a type 202 DISPLEX closed-cycle helium refrigerator mounted on a type 512 HUBER four circle diffractometer. The space group was R3m both at room temperature and at 11 K. The data collection lasted six weeks. Half a sphere of data was collected out to $\sin\theta/\lambda \leq 1.02$ Å. The intensities were normalized to those of the standard reflections and corrected for absorption, Lorentz and polarization effects. Of the 1486 unique reflections collected, 1442 were measured at least three times and the resulting data set seems to be of a high quality,[19] comparable to that of to the data used for the evaluation of the dipole moment in L-alanin.[20, 21]

After finishing the data collection the cell dimensions were monitored while the crystal was heated slowly to room temperature, Figure 5. Further experimental details are given in Table 5.

Neutron study: Neutron powder diffraction measurements were carried out on 4.19 g phosphangulene powder in a vanadium tube using the multidetector powder diffractometer at the DR3 reactor at Risø National Laboratory.[22] The 20 detectors cover the range from 10° to 115.76° in 2θ. To obtain both optimal crystallographic resolution and optimal resolution of the peaks, data were collected at three different monochromator settings. Nine powder diffraction patterns were collected using a neutron beam scattered by the (711) planes of a Ge monochromater, 6 using the (511) and 12 using the (311) planes, respectively. The scattering angle for the monochromator was 90°. The corresponding wavelengths are quoted in Table 6. Subsequently the powder patterns were summed to three separate powder patterns to improve the signal to noise ratio. All three powder patterns were refined simultaneously by the Rietveld method using the program GSAS.[23] Because the vertical divergence of the incident and scattered beam gives rise to an asymmetric peak shape, that is especially difficult to fit well at low diffraction angles, only data in the range from 24° to 115.76° were included in the refinement. The small crystallites of the phosphangulene powder are needle shaped with the polar axis aligned with the needle axis (see also Figure 6), which means that they have a strong tendency to align. As solid phosphangulene is too soft to be ground in a

Table 5. Experimental details. Single crystal X-ray study.

Crystal data	X-ray study
chemical formula	$C_{18}H_9PO_3$
chemical formula weight	304.22
space group	trigonal *R*3m
a,*b* [Å]	16.654(1)
c [Å]	4.166(1)
α,β [°]	90
γ [°]	120
volume [Å]	1000.7(3)
Z	3
D_x [g cm^{-3}]	1.514
radiation	$Ag_{K\alpha}$
wavelength [Å]	0.5594
No. of reflections for cell	68
θ range for cell reflections [°]	24 – 28.4
μ [mm^{-1}]	0.0905
temperature [K]	11(1)
crystal morphology	Colorless crystal bounded by [100] 0.15 mm, [120] – [−120] 0.25 mm [001] 0.6 mm
Data collection	
diffractometer	Type 512 HUBER
scan method	ω-2θ
transmission factors	0.977 – 0.987
No. of measured reflections	10840
No. of unique reflections	1486
R_I [%]	1.75
range *h*,*k*,*l*	$h = \pm 33$, $k = \pm 33$, $l = -8,6$
No. of standards	3 [6,0,0][−6,6,0][6,0,3]
frequency of standards	every 50 reflections
intensity decay [%]	0
refinement on	F^2
$R(F)$,$R(F^2)$ [%]	1.53, 2.18
$Rw(F)$, $Rw(F^2)$ [%]	1.79, 3.71
GoF	1.18
$N_{obs}\ I > 2\sigma(I)$	1457
N_{par}	129
$N_{obs/par}$	11.3
weighting scheme	$1/\sigma(F^2)$

Table 6. Experimental details. Powder neutron study.

Crystal data	Neutron study
a, *b* [Å]	16.654(3)
c [Å]	4.166(3)
wavelengths [Å]	1.126 (Ge(711)), 1.548 (Ge(511)), 2.425 (Ge(311))
temperature [K]	11.0(5)
pattern range [°2θ]	24 – 115.76
No. of profile points	1832
No. reflections	443, 174, 49
No. of parameters refined	76
R_p [%] individual diagrams	1.98, 1.84, 1.51
R_p [%] total	1.74
R_{wp} [%] individual diagrams	2.52, 2.62, 2.69
R_{wp} [%] total	2.62

0947-6539/00/0610-1802 $ 17.50+.50/0 *Chem. Eur. J.* **2000**, *6*, No. 10

mortar a preferred orientation effect must be expected in the powder sample. A correction was included in the refinement. The wavelengths were refined by fixing the cell constants to the values obtained in the X-ray experiment. Further experimental details are given in Table 6. Finally the full structure was refined with isotropic displacement parameters on all atoms. The atomic co-ordinates are given as supplementary material.

ab initio Computations: The calculations were based on a density functional theory (DFT) approach[24] and were carried out with the Gaussian 94 program.[25] The DFT calculations used Becke's three parameter hybrid exchange functional (B3)[26] and the Lee–Yang–Parr (LYP) correlation function.[27] The molecule was constrained to the experimental C_{3v} symmetry and a geometry optimization with the cc-pVDZ basis set[28] was carried out, employing a total of 357 basis functions. Dipole moments were calculated both at the optimized and at the experimental geometries.

Models and refinements: A number of different multipolar models, Equation (3), were tested. In the following eight, that differ mainly in the radial flexibility of the multipoles, will be presented. The models are numbered A–H and the derived dipole moments are listed in Table 7, which also shows agreement factors of the refinement.

Table 7. Multipolar derived dipole moments.

Model	Dipole moment (D)	$Rw(F^2)$ (%)
A	−20.4(31)	3.78
B	−9.9(40)	3.75
C	−7.6(45)	3.73
D	−5.5(44)	3.73
E	−5.4(41)	3.73
F	−4.6(45)	3.71
G	−4.6(28)	3.71
H	−4.7(25)	3.71

The eight models differ as follows:

(A) For the phosphorous, carbon, and oxygen atoms both the core and valence scattering factors were calculated from Hartree–Fock wave functions.[29] A multipole expansion up to the hexadecapole level was used on the phosphorous atom. On the carbon and oxygen atoms expansions up to octapole level were introduced. All the heavy atoms were given a κ expansion/contraction parameter for the spherical monopole term. The radial dependencies of the carbon atoms were constrained to be equal and all κ' were kept equal to 1. In this refinement no information from the neutron study was introduced. Instead the hydrogen atoms were constrained to have the average $C_{aromatic}$–H distance (1.08 Å)[30] in the refined directions. The isotropic displacement parameters of the hydrogens were set to 1.2 times the equivalent isotropic displacement parameters of the carbon atoms to which they are bonded. The SDS scattering factors[31] were used for the hydrogens and neither the κ nor the κ' were refined. (B) A common κ parameter was also refined on the hydrogen atoms. In model (C) the κ' were refined on all heavy atoms but the radial dependencies of the four independent carbon atoms were still constrained to be equal. In model (D) the κ' was refined also on the hydrogen atoms.

The dipole moments derived from models A–D range from −20.4 D to −5.5 D, which demonstrates how large the dependency of the derived dipole moment is on the modeling of hydrogen pseudo-atoms. Therefore positional and isotropic displacement parameters from the neutron study were introduced The Rietveld refinement gave bond lengths of $d_{C(3)-H(2)} = 1.08(1)$ and $d_{C(4)-H(1)} = 1.06(1)$. The isotropic ADP's were found to $Uiso(H(1)) = 0.022(2)$ Å^2 and $Uiso(H(2)) = 0.025(2)$ Å^2.

Model (E) was the same as (D) except that the positional and atomic displacement parameters for the hydrogen atoms were fixed to those obtained in the neutron diffraction study. In model (F) further radial flexibility was introduced by allowing all the carbon κ parameters to change independently of each other. The κ' parameters were still constrained to be equal.

At this point it was found that introducing further radial flexibility into the model led to the κ' refining to nonsensibel results, a behavior typical of a set of least squares equations with an ill-conditioned normal matrix. For this reason the method of singular value decomposition (SVD)[8, 9, 32] was introduced for solving the normal equations. Eigenvalues less than 5×10^{-8} times the largest eigenvalue of the normal matrix were set to zero.

Model (G) was the same as (F) except that SVD was used to solve the normal equations. Solving the least-squares equations by SVD does introduce some mathematical constraints into the model that may not make chemical sense. It is therefore important that the derived dipole moment was found to be −4.6 D, the same as what was obtained with model (F). In the final model (H) also the κ' values on the carbon atoms were allowed to vary independently of each other. The final dipole moment was found to be −4.7(25) D.

As seen above the derived dipole moment shows a large degree of model dependency. It is therefore important to note that dipole moment seems to converge as the radial flexibility of the model is improved. Furthermore the dipole moment is almost exactly the same for models (F), (G), and (H), which have identical $Rw(F^2)$ factor and therefore the data cannot statistically distinguish which model is the best. Also a model with the n values in the exponent of the Slater radial function, Equation (4), that were recommended by Moss et al.[33] on phosphorous was tested. But as the κ' parameters have been refined separately on phosphorous in the present study, this had no effect on the dipole moment.

[1] Entire issues of *Acc. Chem. Res.* **1999**, *32*, and *J. Mater. Chem.* **1999**, *9*, Issue 9.
[2] D. Y. Curtin, I. C. Paul, *Chem. Rev.* **1981**, *81*, 525–541.
[3] J. Sworakowski in *Molecular Electronics* (Ed.: G. J. Ashwell), Research Studies Press, Somerset, **1992**.
[4] F. C. Krebs, P. S. Larsen, J. Larsen, C. S. Jacobsen, C. Boutton, N. Thorup, *J. Am. Chem. Soc.* **1997**, *119*, 1208–1216.
[5] M. A. Spackman, *Chem. Rev.* **1992**, *92*, 1769–1797.
[6] M. A. Spackman, P. G. Byrom, *Acta Crystallogr. Sect. B* **1996**, *52*, 1023–1035.
[7] A. El Haouzi, N. K. Hansen, C. Le Hénaff, J. Protas, *Acta Crystrallogr. Sect. A* **1996**, *52*, 291–301.
[8] M. A. Spackman, P. G. Byrom, *Acta Crystallogr. Sect. B* **1997**, *53*, 553–564.
[9] T. Koritsanszky, S. Howard, P. R. Mallinson, Z. Su, T. Richter, N. K. Hansen, *XD*, *A computer program package for multipole refinement and analysis of charge densities from diffraction data*, **1995**.
[10] P. Coppens, *X-ray Charge Densities and Chemical Bonding*, Oxford University Press, **1997**.
[11] S. T. Howard, M. B. Hursthouse, C. W. Lehmann, P. R. Mallinson, C. S. Frampton, *J. Chem. Phys.* **1992**, *97*, 5616–5630.
[12] In the present work we report s.u.'s as one e.s.d. The original paper on phosphangulene[4] reported s.u.'s as two e.s.d.
[13] M. A. Spackman, P. G. Byrom, M. Alfredsson, K. Hermansson, *Acta Crystallogr. Sect. A* **1999**, *55*, 30–47.
[14] G. K. H. Madsen, B. B. Iversen, F. K. Larsen, M. Kapon, G. M. Reisner, F. H. Herbstein, *J. Am. Chem. Soc.* **1998**, *120*, 10040–10045.
[15] G. K. H. Madsen, C. Wilson, T. M. Nymand, G. J. McIntyre, F. K. Larsen, *J. Phys. Chem. A* **1999**, *103*, 8684–8690.
[16] A. Gavezzotti, *Acc. Chem. Res.* **1994**, *27*, 309–314.
[17] A. Faldt, F. C. Krebs, N. Thorup, *J. Chem. Soc. Perkin Trans. 2* **1997**, 2219–2227.
[18] P. Coppens, Yu. Abramov, M. Carducci, B. Korjov, I. Novozhilova, C. Alhambra, M. R. Pressprich, *J. Am. Chem. Soc.* **1999**, *121*, 2585–2593.
[19] F. K. Larsen, *Acta Crystallogr. Sect. B* **1995**, *51*, 468–482.
[20] R. Destro, R. E. Marsh, R. Bianchi, *J. Phys. Chem.* **1988**, *92*, 966–973.
[21] R. Destro, R. Bianchi, G. Morosi, *J. Phys. Chem.* **1989**, *93*, 4447–4457.
[22] J. Als-Nielsen, N. H. Andersen, C. Broholm, K. N. Clausen, B. Lebech, *The multi Detector Powder Neutron Diffractometer at Risø National Laboratory*, *Risø M2720*, Roskilde, Denmark, **1988**.
[23] A. Larson, R. B. von Dreele, *GSAS: Generalized Structure Analysis System*, Los Alamos National Laboratory, Los Alamos, NM, **1985**.
[24] W. Kohn, A. D. Becke, R. G. Parr, *J. Phys. Chem.* **1996**, *100*, 12974–12980.
[25] M. J. Frisch, G. W. Trucks, H. B. Schlegel, P. M. W. Gill, B. G. Johnson, M. A. Robb, J. R. Cheeseman, T. Keith, G. A. Petersson, J. A. Montgomery, K. Raghavachari, M. A. Al-Laham, V. G. Zakrzewski, J. V. Ortiz, J. B. Foresman, J. Cioslowski, B. B. Stefanov, A. Nanayakkara, M. Challacombe, C. Y. Peng, P. Y. Ayala, W. Chen, M. W. Wong,

J. L. Andres, E. S. Replogle, R. Gomperts, R. L. Martin, D. J. Fox, J. S. Binkley, D. J. Defrees, J. Baker, J. P. Stewart, M. Head-Gordon, C. Gonzalez, J. A. Pople, *Gaussian 94, Revision E. 2*, Pittsburgh PA, **1995**.
[26] A. D. Becke, *J. Chem. Phys.* **1993**, *98*, 5648 – 5652.
[27] C. Lee, W. Yang, R. G. Parr, *Phys. Rev. B* **1988**, *37*, 785 – 789.
[28] T. H. Dunning, Jr., *J. Chem. Phys.* **1989**, *90*, 1007 – 1023.
[29] E. Clementi, C. Roetti, *At. Data Nucl. Data Tables* **1974**, *14*, 177 – 478.
[30] F. H. Allen, O. Kennard, D. G. Watson, L. Brammer, A. G. Orpen, R. Taylor, *Vol. C* (Ed.: A. J. C. Wilson), *International Tables of Crystallography*, **1992**, pp. 685 – 706.
[31] R. F. Stewart, E. R. Davidson, K. T. Simpson, *J. Chem. Phys.* **1965**, *42*, 3175 – 3187.
[32] W. H. Press, S. A. Teukolsky, W. T. Vetterling, B. P. Flannery, *Numerical Recipes*, Cambridge University Press, **1992**.
[33] G. R. Moss, M. Souhassou, R. H. Blessing, E. Espinosa, C. Lecomte, *Acta Crystallogr. Sect. B* **1995**, *51*, 650 – 660.

Received: August 9, 1999 [F1964]

  0947-6539/00/0610-1804 $ 17.50+.50/0